IEEE Access
Multidisciplinary | Rapid Review | Open Access Journal

Received 17 September 2022, accepted 4 October 2022, date of publication 10 October 2022, date of current version 20 October 2022.

Digital Object Identifier 10.1109/ACCESS.2022.3213707

RESEARCH ARTICLE

Extended α-η-μ Fading Distribution: Statistical Properties and Applications

HUSSIEN AL-HMOOD[1], (Member, IEEE), RAFED SABBAR ABBAS[2], AND HAMED AL-RAWESHIDY[3], (Senior Member, IEEE)

[1]Electrical and Electronic Engineering (EEE) Department, University of Thi-Qar, Nasiriyah, Iraq
[2]Department of Electrical Engineering, Faculty of Engineering, University of Kufa, Kufa 540011, Iraq
[3]Department of Electronic and Electrical Engineering, Brunel University London, Uxbridge, UB8 3PH London, U.K.

Corresponding author: Hamed Al-Raweshidy (hamed.al-raweshidy@brunel.ac.uk)

ABSTRACT In this paper, the impact of the non-linearity of the propagation medium on the extended η-μ fading distribution is studied. In particular, the extended α-η-μ fading model in which the parameter α represents the non-linearity of the propagation environment is presented via providing the exact and asymptotic of the statistical properties, namely, the probability density function (PDF), cumulative distribution function (CDF), and generalized-moment generating function (G-MGF). To this effect, exact closed-form mathematically tractable expressions of the outage probability (OP), average symbol error probability (ASEP), amount of fading (AoF), channel quality estimation index (CQEI) and effective rate (ER) are obtained. The asymptotic behaviour at high average signal-to-noise (SNR) values is also analysed to gain further insights into the influence of the index α on the performance metrics of the wireless communication systems. Moreover, the average channel capacity (ACC) under different adaptive transmission techniques, such as, optimum rate and adaptation (ORA), capacity of the channel with inversion and fixed rate (CIFR), and truncated inversion and fixed rate (TIFR) are derived. The validation of the derived expressions is verified via comparing the numerical results with the Monte-Carlo simulations as well as some previous works for different scenarios.

INDEX TERMS Extended α-η-μ fading, statistical properties, outage probability, average symbol error probability, effective rate, average channel capacity.

I. INTRODUCTION

The κ-μ, η-μ [1], and α-μ [2] distributions have been widely utilised to model the multipath fading of the wireless communications channels. This is because these fading models unify most of the classical distributions, namely, Rayleigh, Nakagami-*m*, and Rician, but with better fitting to the realistic measurements.

Recently, several models of the η-μ fading that is used for non-line-of-sight (NLoS) communications scenario have been reported in the technical literature. For instance, the statistical characterization of the composite η-μ/ Gamma fading channel was derived in [3]. The probability density function (PDF) and cumulative distribution function (CDF) of both the signal envelope and instantaneous signal-to-noise ratio (SNR) of α-η-μ distribution were given in [4]. The performance of the wireless digital communications systems over α-η-μ fading model in terms of the outage probability (OP), average symbol error probability (ASEP) for various modulation schemes, and average channel capacity (ACC) was studied in [5] and [6]. The average probability of energy detection based spectrum sensing over α-η-μ fading channels was derived in [7]. Moreover, the effective rate (ER), i.e. capacity, in α-η-μ fading condition was given in [8]. The authors of [9] analysed the physical layer security over α-η-μ fading scenario in terms of the lower bound secure outage probability (SOP). In [10], the ACC of a mobile user over α-η-μ fading channel was investigated via employing the random waypoint (RWP) mobility approach. The composite of α-η-μ/Gamma and α-η-λ-μ/Gamma distributions were

The associate editor coordinating the review of this manuscript and approving it for publication was Xiaofan He.

investigated in [11] and [12], respectively, with applications to the ACC with optimum rate adaptation (ORA) and constant transmit power, channel inversion with fixed rate (CIFR), and truncated inversion and fixed rate (TIFR) adaptive transmission protocols. The α-η-κ-μ fading model was suggested in [13] as a unified representation for both α-η-μ and κ-μ distributions. Additionally, the main advantage of this model is manifested in providing better fitting to the empirical data in a mmWave propagation medium than Rayleigh, Rice, Nakagami-m, α-μ, η-μ and κ-μ distributions [14]. Consequently, the expressions of the ER of α-η-κ-μ fading channel of the single and multiple inputs wireless communication systems were provided in [15] and [16], respectively.

More recently, the authors in [17] proposed the extended η-μ distribution via assuming the clustering imbalance between the in-phase and quadrature components. In addition, this model includes the classical η-μ distribution which unifies number of the conventional distributions, as a special case (see [17] and the references therein). Furthermore, the fundamental statistics of the extended η-μ fading condition are given in simple and closed-form expressions in comparison with the α-η-κ-μ fading model in which the imbalance between the clustering of the in-phase and quadrature components is also considered. Accordingly, the PDF, CDF, and moment generating function (MGF) of the sum and maximum of the extended η-μ variates were derived in [18] and [19], respectively, with applications to diversity combining techniques. The success and outage probabilities of amplify-and-forward relay-aided device-to-device (D2D) communication system were reported in [20]. The OP, ASEP, ACC, and amount of fading (AoF) over the extended η-$\mathcal{F}$ fading which is composite of the extended η-μ and inverse Nakagami-m distributions were provided in [21].

Based on the above advantages of the extended η-μ fading distribution and taking into consideration the impact of the non-linearity propagation environment on the transmitted signal power, the extended α-η-μ fading model is proposed in this paper. Therefore, this model comprises the NLoS communication scenario that is modelled by the η-μ fading distribution, the non-linearity of the propagation environment and imbalance between the clustering of the in-phase and quadrature components simultaneously. To this end and unlike [13], the statistical properties and important performance metrics of wireless communications systems are provided in exact closed-form analytically tractable expressions. Furthermore, several exact and asymptotic expressions of the performance measurements of the wireless communications systems are derived.

The main contributions are summarized as follows:

- Deriving the PDF, CDF, and generalised-MGF (G-GMF) of both the envelope and instantaneous signal-to-noise ratio (SNR) over extended α-η-μ fading distribution in novel exact closed-form mathematically acceptable formats. To the best of the authors' knowledge, there is no effort in the state-of-the-art has been dedicated to study the effect of the non-linearity of the propagation media on the extended η-μ distribution.
- Providing the asymptotic expressions of the derived statistics at high average SNR regime to get more insights into the influence of the fading indices on the system behaviour.
- Using the above statistical properties, the performance of the wireless communication systems over extended α-η-μ fading channel is analysed in terms of the OP, ASEP, AoF, channel quality estimation index (CQEI) and ER. To this effect, both the exact and asymptotic expressions of the performance metrics are novel, simple and computationally tractable.
- Studying the ACC over extended α-η-μ fading channels with different adaptive transmission strategies. In particular, the average capacity of channel with ORA and constant transmit power, CIFR, and TIFR transmission strategies are studied.

Organization: Section II provides some fundamental information about the extended η-μ fading distribution. In Section III, the the principle work of the proposed α-η-μ fading distribution is explained as well as the statistical properties of this model are given. Section IV analyses the performance of wireless communications systems in terms of the OP, ASEP, AoF, and ER. In this section, the ACC under ORA, CIFR, and TIFR transmission techniques are also derived. Section V presents the Monte Carlo simulations and numerical results for different scenarios. Section VI highlights some conclusion remarks about the proposed model.

Notations: $\mathbb{E}[.]$ denotes the statistical expectation, $\Gamma(.)$ is the gamma function [22, eq. (8.310.1)], ${}_1F_1(.;.;.)$ represents the confluent hypergeometric function [22, eq. (9.14.1)], $H_{c,d}^{a,b}[.]$ refers to the Fox's H-function (FHF) [23, eq. (1.2)], $H_{m,n:p,q;r,s}^{a,b:c,d;e,f}[.]$ stands for the bivariate FHF (BFHF) defined in [23, eq. (2.57)] that can be calculated by using the MATLAB code of [24], $i = \sqrt{-1}$, $\mathrm{erfc}(x)$ is the complementary error function [22, eq. (8.250.4)], $G_{c,d}^{a,b}[.]$ is the Meijer's G-function (MGF) [23, eq. (1.111)], ${}_2F_1(.,.;.;.)$ represents the Gauss hypergeometric function [22, eq. (9.14.2)], and $B(a,b)$ denotes the beta function defined in [22, eq. (8.380.1)].

II. THE EXTENDED η-μ FADING MODEL

The received signal envelope for the extended η-μ fading distribution, $R_{E\eta\mu}$, is given by [17]

$$R_{E\eta\mu}^2 = \sum_{l=1}^{\mu_x} X_l^2 + \sum_{l=1}^{\mu_y} Y_l^2 \tag{1}$$

where μ_x and μ_y are the number of the multipath clusters of the in-phase and quadrature components, respectively, whereas X_l^2 and Y_l^2 that are mutually independent Gaussian RVs with zero mean, namely, $\mathbb{E}[X_l] = \mathbb{E}[Y_l]$, represent the in-phase and quadrature components of the cluster l, respectively.

The PDF of $R_{E\eta\mu}$, $f_{R_{E\eta\mu}}(r)$, is expressed as [17, eq. (14)]

$$f_{R_{E\eta\mu}}(r) = \frac{2(\mu\xi)^{\mu}}{\Gamma(\mu)}\left(\frac{p}{\eta}\right)^{\frac{\mu p}{1+p}} \frac{r^{2\mu-1}}{\hat{r}^{2\mu}} \exp\left(-\frac{\mu\xi r^2}{\hat{r}^2}\right) \times {}_1F_1\left(\frac{\mu p}{1+p}; \mu; \frac{\mu\xi(\eta-p)r^2}{\eta\hat{r}^2}\right) \quad (2)$$

where $\mu = (\mu_x + \mu_y)/2$ stands for the total number of the multipath clusters, $\hat{r}^2 = \mathbb{E}[R^2_{E\eta\mu}]$ is the average power of the fading envelope, the parameter p indicates the clustering imbalance between the in-phase and quadrature components, $\xi = (1+\eta)/(1+p)$.

Similar to the η-μ fading model, the extended η-μ distribution encompasses two formats. In Format I, p represents the ratio between the number of the multipath clusters of the components, namely, $p = \mu_x/\mu_y$ with $\mu_x = 2\mu p/(1+p)$ and $\mu_y = 2\mu/(1+p)$. Moreover, η is the ratio of the powers of the in-phase and quadrature components, i.e., $\eta = \Omega_x/\Omega_y$ $(0 < \eta < \infty)$ with $\Omega_x = \mathbb{E}[X_l^2] = 2\eta\hat{r}^2/(1+\eta)$ and $\Omega_y = \mathbb{E}[Y_l^2] = 2\hat{r}^2/(1+\eta)$. On the other side, in Format II, p stands for the normalized difference of the number of the multipath clusters of the in-phase and quadrature components, namely, $p = (\mu_x - \mu_y)/(\mu_x + \mu_y)$ with $\mu_x = (1+p)\mu$ and $\mu_y = (1-p)\mu$. Furthermore, $\eta = (\Omega_x - \Omega_y)/(\Omega_x + \Omega_y)$ $(-1 < \eta < 1)$ that means η represents the normalized difference of the powers of the multipath clusters with $\Omega_x = (1+\eta)\hat{r}^2$ and $\Omega_x = (1-\eta)\hat{r}^2$. It is worth mentioning that Format I and Format II are related to each other by $\eta_{\rm I} = (1+\eta_{\rm II})/(1-\eta_{\rm II})$ and $p_{\rm I} = (1+p_{\rm II})/(1-p_{\rm II})$. Hence, Format I is used in this work.

III. THE EXTENDED α-η-μ FADING DISTRIBUTION

In this section, the extended α-η-μ fading distribution is proposed via adding the impact of the non-linearity of the propagation medium that is represented by the parameter α. Interestingly, this distribution comprises several models as particular cases, such as, α-μ and extended η-μ distributions. The former model is obtained via inserting $p = \eta$ or $p = 1$ and a specific value for η whereas the latter arises by making $\alpha = 2$. In addition to that, the extended α-μ fading model that has not been yet reported by the previous works, can be also considered as special case of the α-η-μ fading distribution. All the special cases of the α-η-μ fading and the corresponding values of their fading parameters p, α, η, and μ are described in Table 1.

A. PDF OF THE EXTENDED α-η-μ DISTRIBUTION

Theorem 1: Let $\alpha, \eta, \mu, p, \hat{r}^{\alpha}, r \in \mathbb{R}^+$ where r is a random variable (RV) that denotes the instantaneous signal power of the fading envelope, R, of the extended α-η-μ distribution. Accordingly, the PDF of envelope, R, can be expressed as

$$f_R(r) = \frac{\alpha\phi^{\mu}}{\Gamma(\mu)}\left(\frac{p}{\eta}\right)^{\frac{\mu p}{1+p}} \frac{r^{\alpha\mu-1}}{\hat{r}^{\alpha\mu}} \exp\left(-\phi\frac{r^{\alpha}}{\hat{r}^{\alpha}}\right) \times {}_1F_1\left(\frac{\mu p}{1+p}; \mu; \frac{\phi(\eta-p)r^{\alpha}}{\eta\hat{r}^{\alpha}}\right) \quad (3)$$

TABLE 1. Common fading channels extracted from the extended α-η-μ distribution.

Fading Channels	Extended α-η-μ Fading Parameters
α-η-μ [4]	$p = 1, \underline{\alpha} = \alpha, \underline{\eta} = \eta, \underline{\mu} = \mu$
η-μ [1]	$p = 1, \underline{\alpha} = 2, \underline{\eta} = \eta, \underline{\mu} = \mu$
Extended η-μ [17]	$\underline{p} = p, \underline{\alpha} = 2, \underline{\eta} = \eta, \underline{\mu} = \mu$
Extended α-μ	$\underline{p} = p, \underline{\alpha} = \alpha, \underline{\eta} = 1, \underline{\mu} = \mu$
α-μ [2]	$\underline{p} = \eta, \underline{\alpha} = \alpha, \underline{\eta} = p, \underline{\mu} = \mu$
Nakagami-m [1], [2]	$\underline{p} = \eta, \underline{\alpha} = 2, \underline{\eta} = p, \underline{\mu} = m$
Rayleigh [1], [2]	$\underline{p} = \eta, \underline{\alpha} = 2, \underline{\eta} = p, \underline{\mu} = 1$
One-sided Gaussian [1], [2]	$\underline{p} = \eta, \underline{\alpha} = 2, \underline{\eta} = p, \underline{\mu} = 0.5$

where

$$\phi = \left(\frac{\Gamma(\mu+\frac{2}{\alpha}){}_1F_1\left(\frac{\mu p}{1+p}; \mu+\frac{2}{\alpha}; \frac{\eta-p}{\eta}\right)}{\Gamma(\mu)\left(\frac{\eta}{p}\right)^{\frac{\mu p}{1+p}}}\right)^{\frac{\alpha}{2}}. \quad (4)$$

Proof: The envelope R can be written as

$$R^{\alpha} = \sum_{l=1}^{\mu_x} X_l^2 + \sum_{l=1}^{\mu_y} Y_l^2. \quad (5)$$

Comparing (1) with (5), one can deduce that

$$R^{\alpha} = R^2_{E\eta\mu}. \quad (6)$$

Now, let's define the received signal power of the fading envelope of the extended η-μ fading as

$$\chi_{E\eta\mu} = R^2_{E\eta\mu}. \quad (7)$$

Employing the transformation of the RV of (7) in (2), this yields

$$f_{\chi_{E\eta\mu}}(x) = \frac{(\mu\xi)^{\mu}}{\Gamma(\mu)}\left(\frac{p}{\eta}\right)^{\frac{\mu p}{1+p}} \frac{x^{\mu-1}}{\hat{r}^{2\mu}} \exp\left(-\frac{\mu\xi x}{\hat{r}^2}\right) \times {}_1F_1\left(\frac{\mu p}{1+p}; \mu; \frac{\mu\xi(\eta-p)x}{\eta\hat{r}^2}\right) \quad (8)$$

where $\hat{r}^2 = \mathbb{E}[\chi_{E\eta\mu}]$.

The instantaneous signal power of the envelope, r, under α-η-μ distribution can be found using

$$r^2 = \frac{\hat{r}^2 R^2}{\mathbb{E}[R^2]} = \frac{\hat{r}^2 \chi^{2/\alpha}_{E\eta\mu}}{\mathbb{E}[\chi^{2/\alpha}_{E\eta\mu}]}. \quad (9)$$

To compute $\mathbb{E}[\chi^{2/\alpha}_{E\eta\mu}]$, we need to find the k-th moment of the RV $\chi_{E\eta\mu}$, namely, $\chi^k_{E\eta\mu}$, of the extended $\eta-\mu$ distribution. Hence, utilising (8) and [22, eq. (7.522.9)], we have

$$\mathbb{E}[\chi^k_{E\eta\mu}] = \frac{\Gamma(\mu+k)\left(\frac{\hat{r}^2}{\mu\xi}\right)^k\left(\frac{p}{\eta}\right)^{\frac{\mu p}{1+p}}{}_1F_1\left(\frac{\mu p}{1+p}; \mu+k; \frac{\eta-p}{\eta}\right)}{\Gamma(\mu)}. \quad (10)$$

Substituting $k = 2/\alpha$ into (10), using the concept of transformation of RVs and then inserting the result in

$$f_R(r) = \frac{\alpha r^{\alpha-1}}{\hat{r}^{\alpha}}\left(\mathbb{E}\left[\chi^{2/\alpha}_{E\eta\mu}\right]\right)^{2/\alpha} f_{\chi_{E\eta\mu}}\left(\frac{r^{\alpha}}{\hat{r}^{\alpha}}\mathbb{E}\left[\chi^{2/\alpha}_{E\eta\mu}\right]\right). \quad (11)$$

Additionally, doing some mathematical straightforward simplifications, (3) is obtained which completes the proof. ■

Lemma 1: Assume $\gamma \in \mathbb{R}^+$ be a RV that represents the instantaneous SNR under the extended α-η-μ fading channel with average $\bar{\gamma} = \mathbb{E}[\gamma]$. Thus, the exact PDF of γ, $f_\gamma(\gamma)$, and its asymptotic expression when $\bar{\gamma} \to \infty$, $f_\gamma^\infty(\gamma)$, are given, respectively, by

$$f_\gamma(\gamma) = \frac{\alpha\phi^\mu}{2\Gamma(\mu)}\left(\frac{p}{\eta}\right)^{\frac{\mu p}{1+p}} \frac{\gamma^{\frac{\alpha\mu}{2}-1}}{\bar{\gamma}^{\frac{\alpha\mu}{2}}} \exp\left(-\phi\frac{\gamma^{\frac{\alpha}{2}}}{\bar{\gamma}^{\frac{\alpha}{2}}}\right) \times {}_1F_1\left(\frac{\mu p}{1+p}; \mu; \frac{\phi(\eta-p)\gamma^{\frac{\alpha}{2}}}{\eta\bar{\gamma}^{\frac{\alpha}{2}}}\right) \quad (12)$$

and

$$f_\gamma^\infty(\gamma) \simeq \frac{\alpha\phi^\mu}{2\Gamma(\mu)}\left(\frac{p}{\eta}\right)^{\frac{\mu p}{1+p}} \frac{\gamma^{\frac{\alpha\mu}{2}-1}}{\bar{\gamma}^{\frac{\alpha\mu}{2}}}. \quad (13)$$

Proof: Using the concept of transformation between γ and R, i.e., $\gamma = \bar{\gamma}R^2/\mathbb{E}[R^2]$, which leads to $f_\gamma(\gamma) = \sqrt{\hat{r}^2/\bar{\gamma}\gamma} f_R(\sqrt{\gamma\hat{r}^2/\bar{\gamma}})/2$, the result is (12).

Using the fact that both the exponential function and ${}_1F_1(.;.;.)$ tend to unity when $\bar{\gamma} \to \infty$ in (12), (13) is yielded and this finishes the proof. ■

Lemma 2: To avoid the infinite series expressions of the CDF and G-MGF as well as the performance metrics, the PDF of (12) can be rewritten in terms of the product of two univariate FHFs as

$$f_\gamma(\gamma) = \frac{\alpha\phi^\mu}{2\Gamma\left(\frac{\mu\varphi}{1+p}\right)}\left(\frac{p}{\eta}\right)^{\frac{\mu p}{1+p}} \frac{\gamma^{\frac{\alpha\mu}{2}-1}}{\bar{\gamma}^{\frac{\alpha\mu}{2}}} \times H_{0,1}^{1,0}\left[\frac{\phi\delta}{\bar{\gamma}^{\frac{\alpha}{2}}}\gamma^{\frac{\alpha}{2}}\middle|\begin{matrix}-\\(0,1)\end{matrix}\right] \times H_{1,2}^{1,1}\left[\frac{\phi\beta}{\eta\bar{\gamma}^{\frac{\alpha}{2}}}\gamma^{\frac{\alpha}{2}}\middle|\begin{matrix}(1-\frac{\mu\varphi}{1+p},1)\\(0,1),(1-\mu,1)\end{matrix}\right] \quad (14)$$

where $(\varphi, \delta, \beta) = (p, 1, p-\eta)$ for $\eta < p$ whereas $(\varphi, \delta, \beta) = (1, p/\eta, \eta - p)$ for $\eta > p$.[1]

Proof: The exponential function can be written in terms of the FHF via recalling the identity [23, eq. (1.39)]

$$e^{-x} = H_{0,1}^{1,0}\left[x\middle|\begin{matrix}-\\(0,1)\end{matrix}\right]. \quad (15)$$

In addition, the confluent hypergeometric function can be expressed in terms of the FHF via invoking the property [23, eq. (1.130)]

$${}_1F_1(a;b;-x) = \frac{\Gamma(b)}{\Gamma(a)} H_{1,2}^{1,1}\left[x\middle|\begin{matrix}(1-a,1)\\(0,1),(1-b,1)\end{matrix}\right]. \quad (16)$$

Using (15) and (16) in (12), the PDF of the extended α-η-μ distribution for $\eta < p$ is formulated as

$$f_\gamma(\gamma) = \frac{\alpha\phi^\mu}{2\Gamma\left(\frac{\mu p}{1+p}\right)}\left(\frac{p}{\eta}\right)^{\frac{\mu p}{1+p}} \frac{\gamma^{\frac{\alpha\mu}{2}-1}}{\bar{\gamma}^{\frac{\alpha\mu}{2}}} H_{0,1}^{1,0}\left[\frac{\phi}{\bar{\gamma}^{\frac{\alpha}{2}}}\gamma^{\frac{\alpha}{2}}\middle|\begin{matrix}-\\(0,1)\end{matrix}\right] \times H_{1,2}^{1,1}\left[\frac{\phi(p-\eta)}{\eta\bar{\gamma}^{\frac{\alpha}{2}}}\gamma^{\frac{\alpha}{2}}\middle|\begin{matrix}(1-\frac{\mu p}{1+p},1)\\(0,1),(1-\mu,1)\end{matrix}\right]. \quad (17)$$

[1]For the case $\eta = p$, ${}_1F_1(.;.;0) = 1$ and (12) reduces to the PDF of γ over $\alpha - \mu$ fading model [2].

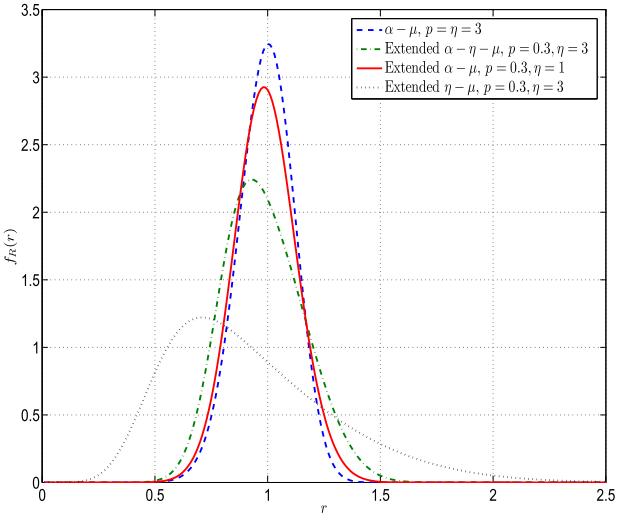

FIGURE 1. Envelope PDF for different cases of extended α-η-μ fading with $\alpha = 4.5$, $\mu = 3.5$ and $\hat{r} = 1$.

It is worth noting that (17) is not applicable for $\eta > p$ because the integral of the FHF converges when the arguments are positive. Consequently, the property that is given in (16) can be used after recalling the identity ${}_1F_1(a;b;x) = e^x {}_1F_1(b-a;b;-x)$ [22, eq. (9.212)]. Thus, this yields

$$f_\gamma(\gamma) = \frac{\alpha\phi^\mu}{2\Gamma\left(\frac{\mu}{1+p}\right)}\left(\frac{p}{\eta}\right)^{\frac{\mu p}{1+p}} \frac{\gamma^{\frac{\alpha\mu}{2}-1}}{\bar{\gamma}^{\frac{\alpha\mu}{2}}} H_{0,1}^{1,0}\left[\frac{\phi p}{\eta\bar{\gamma}^{\frac{\alpha}{2}}}\gamma^{\frac{\alpha}{2}}\middle|\begin{matrix}-\\(0,1)\end{matrix}\right] \times H_{1,2}^{1,1}\left[\frac{\phi(\eta-p)}{\eta\bar{\gamma}^{\frac{\alpha}{2}}}\gamma^{\frac{\alpha}{2}}\middle|\begin{matrix}(1-\frac{\mu}{1+p},1)\\(0,1),(1-\mu,1)\end{matrix}\right]. \quad (18)$$

One can notice that both (17) and (18) can be unified in a single format with three different parameters as in (14) and this completes the proof. ■

Fig. 1 illustrates the PDF of the envelope of extended $\alpha - \eta - \mu$ fading with $\alpha = 4.5$ and $\mu = 3.5$. From this figure, one can see that the increasing in α from 2 (extended η-μ) to 4.5 (extended α-η-μ) leads to increase the PDF as well as shift it rightwards which means better fading scenario. In the same context, when p decreases from 3 to 0.3, the PDF reduces and shifts leftwards. Fig. 1 also demonstrates some special cases of the extended α-η-μ fading distribution that are explained in Table 1.

B. CDF OF THE EXTENDED α-η-μ DISTRIBUTION

Theorem 2: The CDF of R, $F_R(r)$, and the CDF of γ, $F_\gamma(\gamma)$, under extended α-η-μ fading model can be written in exact closed-form expression as given in (19) and (20), respectively, shown at the bottom of the next page.

The asymptotic of the CDF of (20) at $\bar{\gamma} \to \infty$, $F_\gamma^\infty(\gamma)$, is expressed as

$$F_\gamma^\infty(\gamma) \simeq \frac{\left(\frac{p}{\eta}\right)^{\frac{\mu p}{1+p}}}{\Gamma(1+\mu)}\left(\frac{\phi\gamma^{\frac{\alpha}{2}}}{\bar{\gamma}^{\frac{\alpha}{2}}}\right)^\mu. \quad (21)$$

Proof: Following the same steps in Lemma 2 for (3) and making use of the definition of the FHF [23, eq. (1.2)] that is

given in (22) shown at the bottom of the page in which $\mathcal{T}$ represents the suitable contour in the t-plane from ϱ-$i\infty$ to ϱ+$i\infty$ with ϱ is a constant value, we have (23) as shown at the bottom of the page.

Now, inserting (23) in $F_R(r) = \int_0^r f_R(r)dr$ and changing the order of the integrals, the linear integral can be easily evaluated. Thereafter, doing some mathematical manipulations via using the identity $\Gamma(x+1) = x\Gamma(x)$ [22, eq. (8.331.1)] and invoking [23, eq. (2.57)], (19) is deduced.

Plugging (23) in $f_\gamma(\gamma) = \sqrt{\hat{r}^2/\bar{\gamma}\gamma} f_R(\sqrt{\gamma\hat{r}^2/\bar{\gamma}})/2$, we have (24), as shown at the bottom of the page. Then, substituting (24) into $F_\gamma(\gamma) = \int_0^\gamma f_\gamma(\gamma)d\gamma$ and employing the same procedure of (19), (20) is derived.

Inserting (13) in $F_\gamma^\infty(\gamma) = \int_0^\gamma f_\gamma^\infty(\gamma)d\gamma$ and computing the integral, (21) is obtained and this accomplishes the proof. ■

Fig. 2 shows the envelope CDF of the extended α-η-μ fading model for the same fading parameters of Fig. 1. The results of Fig. 1 are confirmed in Fig. 2 where the increasing in α and/or p would lead to diminish the CDF which refers to better fading condition. Also, a comparison with [2] and [17] for α-μ and extended η-μ, respectively, is also carried out in Fig. 2. As it can be observed, the envelope CDF of (19) is in an excellent matching with the results of the previous works [2] and [17] which verifies the correctness of our derived CDF.

Lemma 3: The exact G-MGF of γ, $\mathcal{M}_\gamma^{(k)}(s)$, under the extended α-η-μ fading distribution can be written in exact closed-form as in (25) shown at the bottom of the page.

The asymptotic of the G-MGF at $\bar{\gamma} \to \infty$ can be expressed as

$$\mathcal{M}_\gamma^{(k),\infty}(s) \simeq \frac{\alpha}{2\Gamma(\mu)}\left(\frac{p}{\eta}\right)^{\frac{\mu p}{1+p}}\left(\frac{\phi}{(s\bar{\gamma})^{\frac{\alpha}{2}}}\right)^{\mu}\frac{\Gamma(\frac{\alpha}{2}\mu+k)}{s^k}. \quad (26)$$

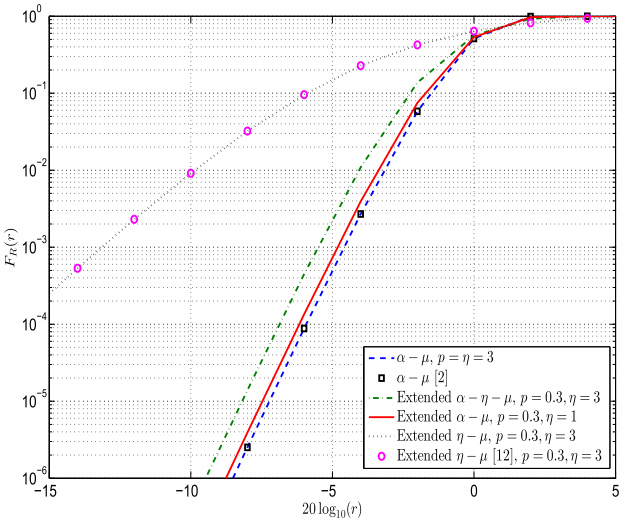

FIGURE 2. Envelope CDF for different cases of extended α-η-μ fading with $\alpha = 4.5$, $\mu = 3.5$ and $\hat{r} = 1$.

Proof: The G-MGF can be evaluated by [25, eq. (2)]

$$\mathcal{M}_\gamma^{(k)}(s) = \mathbb{E}[\gamma^k e^{-s\gamma}] = \int_0^\infty \gamma^k e^{-s\gamma} f_\gamma(\gamma)d\gamma. \quad (27)$$

Substituting (24) into (27) and changing the order of the integrals, (28) is obtained as shown at the bottom of the next page.

Making utilise of [22, eq. (3.381.4)] to compute the linear integral and with the aid of [23, eq. (2.57)], (25) is yielded.

$$F_R(r) = \frac{\alpha\phi^\mu}{2\Gamma(\frac{\mu\varphi}{1+p})}\left(\frac{p}{\eta}\right)^{\frac{\mu p}{1+p}}\frac{r^{\alpha\mu}}{\hat{r}^{\alpha\mu}}H_{1,1:0,1;1,2}^{0,1:1,0;1,1}\left[\frac{\phi\delta}{\hat{r}^\alpha}r^\alpha, \frac{\phi\beta}{\eta\hat{r}^\alpha}r^\alpha\middle|\begin{matrix}(1-\frac{\alpha\mu}{2};\frac{\alpha}{2},\frac{\alpha}{2}):-;(1-\frac{\mu\varphi}{1+p},1)\\(-\frac{\alpha\mu}{2};\frac{\alpha}{2},\frac{\alpha}{2}):(0,1);(0,1),(1-\mu,1)\end{matrix}\right]. \quad (19)$$

$$F_\gamma(\gamma) = \frac{\alpha\phi^\mu}{2\Gamma(\frac{\mu\varphi}{1+p})}\left(\frac{p}{\eta}\right)^{\frac{\mu p}{1+p}}\frac{\gamma^{\frac{\alpha\mu}{2}}}{\bar{\gamma}^{\frac{\alpha\mu}{2}}}H_{1,1:0,1;1,2}^{0,1:1,0;1,1}\left[\frac{\phi\delta}{\bar{\gamma}^{\frac{\alpha}{2}}}\gamma^{\frac{\alpha}{2}}, \frac{\phi\beta}{\eta\bar{\gamma}^{\frac{\alpha}{2}}}\gamma^{\frac{\alpha}{2}}\middle|\begin{matrix}(1-\frac{\alpha\mu}{2};\frac{\alpha}{2},\frac{\alpha}{2}):-;(1-\frac{\mu\varphi}{1+p},1)\\(-\frac{\alpha\mu}{2};\frac{\alpha}{2},\frac{\alpha}{2}):(0,1);(0,1),(1-\mu,1)\end{matrix}\right]. \quad (20)$$

$$H_{p,q}^{m,n}\left[x\middle|\begin{matrix}(a_1,A_1),\cdots,(a_p,A_p)\\(b_1,B_1),\cdots,(b_p,B_p)\end{matrix}\right] = \frac{1}{2\pi i}\int_{\mathcal{T}}\frac{\{\prod_{j=1}^m\Gamma(b_j+B_jt)\}\{\prod_{j=1}^n\Gamma(1-a_j-A_jt)\}}{\{\prod_{j=m+1}^q\Gamma(1-b_j-B_jt)\}\{\prod_{j=n+1}^p\Gamma(a_j+A_jt)\}}x^{-t}dt. \quad (22)$$

$$f_R(r) = \frac{\alpha\phi^\mu}{\Gamma(\frac{\mu\varphi}{1+p})}\left(\frac{p}{\eta}\right)^{\frac{\mu p}{1+p}}\frac{r^{\alpha\mu-1}}{\hat{r}^{\alpha\mu}}\frac{1}{(2\pi i)^2}\int_{\mathcal{T}_1}\int_{\mathcal{T}_2}\frac{\Gamma(t_1)\Gamma(t_2)\Gamma\left(\frac{\mu\varphi}{1+p}-t_2\right)}{\Gamma(\mu-t_2)}\left(\frac{\phi\delta}{\hat{r}^\alpha}r^\alpha\right)^{-t_1}\left(\frac{\phi\beta}{\eta\hat{r}^\alpha}r^\alpha\right)^{-t_2}dt_1dt_2. \quad (23)$$

$$f_\gamma(\gamma) = \frac{\alpha\phi^\mu}{2\Gamma(\frac{\mu\varphi}{1+p})}\left(\frac{p}{\eta}\right)^{\frac{\mu p}{1+p}}\frac{\gamma^{\frac{\alpha\mu}{2}-1}}{\bar{\gamma}^{\frac{\alpha\mu}{2}}}\frac{1}{(2\pi i)^2}\int_{\mathcal{T}_1}\int_{\mathcal{T}_2}\frac{\Gamma(t_1)\Gamma(t_2)\Gamma\left(\frac{\mu\varphi}{1+p}-t_2\right)}{\Gamma(\mu-t_2)}\left(\frac{\phi\delta}{\bar{\gamma}^{\frac{\alpha}{2}}}\gamma^{\frac{\alpha}{2}}\right)^{-t_1}\left(\frac{\phi\beta}{\eta\bar{\gamma}^{\frac{\alpha}{2}}}\gamma^{\frac{\alpha}{2}}\right)^{-t_2}dt_1dt_2. \quad (24)$$

$$\mathcal{M}_\gamma^{(k)}(s) = \frac{\alpha\phi^\mu}{2\Gamma(\frac{\mu\varphi}{1+p})(s\bar{\gamma})^{\frac{\alpha\mu}{2}}s^k}\left(\frac{p}{\eta}\right)^{\frac{\mu p}{1+p}}H_{1,0:0,1;1,2}^{0,1:1,0;1,1}\left[\frac{\phi\delta}{(s\bar{\gamma})^{\frac{\alpha}{2}}}, \frac{\phi\beta}{\eta(s\bar{\gamma})^{\frac{\alpha}{2}}}\middle|\begin{matrix}(1-k-\frac{\alpha\mu}{2};\frac{\alpha}{2},\frac{\alpha}{2}):-;(1-\frac{\mu\varphi}{1+p},1)\\-:(0,1);(0,1),(1-\mu,1)\end{matrix}\right]. \quad (25)$$

TABLE 2. The values of A_1 and A_2 for coherent modulation schemes [27].

Modulation Scheme	A_1	A_2	M
BPSK	0.5	1	-
GMSK	1	B	-
M-DEPSK	2	$\sin^2(\pi/M)$	≥ 2
QPSK	1	0.5	-
M-PSK	1	$\sin^2(\pi/M)$	> 4
M-FSK	$(M-1)/2$	0.5	> 2
Square M-QAM	$2-2/\sqrt{M}$	$\frac{3}{2(M-1)}$	≥ 4
M-DPSK	1	$2\sin^2(\pi/(2M))$	≥ 2

At high $\bar{\gamma}$ regime, the asymptotic of the G-MGF can be calculated via substituting (13) into (27) and using [22, eq. (3.381.4)] to obtain (26). Then, the proof is completed. ■

IV. PERFORMANCE EVALUATION OF WIRELESS COMMUNICATIONS SYSTEMS OVER EXTENDED α-η-μ FADING MODEL

A. OUTAGE PROBABILITY

The probability of reducing the output SNR to less than a certain threshold value, ψ, is called the outage probability. Consequently, the OP, P_o, can be evaluated by [26, eq. (1.4)]

$$P_o = F_\gamma(\psi) \tag{29}$$

where $F_\gamma(.)$ is presented in (20).

The asymptotic of the OP, P_o^∞, can be deduced from (21), i.e., $P_o^\infty = F_\gamma^\infty(\psi)$. Additionally, the P_o^∞ may be expressed as $P_o^\infty \simeq (\mathcal{G}_c\bar{\gamma})^{-\mathcal{G}_d}$ whereby $\mathcal{G}_c$ and $\mathcal{G}_d$ are the diversity order and coding gain, respectively. Hence, one can see that $\mathcal{G}_c = \frac{1}{\psi}\left[\left(\frac{\eta}{p}\right)^{p/(1+p)}\frac{[\Gamma(1+\mu)]^{1/\mu}}{\phi}\right]^{2/\alpha}$ and $\mathcal{G}_d = \alpha\mu/2$. It can be noted that $\mathcal{G}_d$ depends on the fading parameters α and μ.

B. AVERAGE SYMBOL ERROR PROBABILITY

1) NON-COHERENT MODULATION

The ASEP for non-coherent modulation, $\bar{P}_s^N$, can be computed by [26, eq. (1.8)]

$$\bar{P}_s^N = a_1\mathcal{M}_\gamma(a_2) \tag{30}$$

where a_1 and a_2 are the modulation constants that are defined as $(a_1, a_2) = (0.5, 1)$ and $(a_1, a_2) = (0.5, 0.5)$ for differential binary phase shift keying (DBPSK) and non-coherent binary frequency shift keying (NCBFSK) schemes, respectively. Furthermore, for M-ary-non-coherent FSK (M-NFSK) with $M \geq 2$, $a_1 = \sum_{m=1}^{M-1}(-1)^{m+1}/(m+1)$ and $a_2 = m/(m+1)$. In (30), $\mathcal{M}_\gamma(a_2)$ is the MGF of the extended α-η-μ fading that can be obtained from (25) via using $k = 0$ and replacing s by a_2.

Similarly, the asymptotic expression of the ASEP for the non-coherent detection schemes at high $\bar{\gamma}$ values, $\bar{P}_s^{N,\infty}$, can be derived from (30) and (26) after inserting $k = 0$ and $s = a_2$. Hence, one can observe that $\mathcal{G}_d$ is also proportional to α and μ where $\mathcal{G}_d = \alpha\mu/2$ and $\mathcal{G}_c = a_2\left[\left(\frac{\eta}{p}\right)^{p/(1+p)}\left(\frac{2\Gamma(\mu)}{a_1\alpha\phi^\mu\Gamma(\alpha\mu/2)}\right)^{\frac{1}{\mu}}\right]^{2/\alpha}$.

2) COHERENT MODULATION

For coherent modulation schemes, such as, BPSK, for high $\bar{\gamma}$ for Gaussian minimum shift keying (GMSK), M-ary-differentially encoded PSK (M-DEPSK), quadrature PSK (QPSK), M-ary-PSK (M-PSK), M-ary-FSK (M-FSK), square M-ary-quadrature amplitude modulation (M-QAM), and M-ary-differential PSK (M-DPSK), the ASEP, $\bar{P}_s^C$, can be calculated by [27, eq. (19)]

$$\bar{P}_s^C = A_1\int_0^\infty \mathrm{erfc}(\sqrt{A_2\gamma})f_\gamma(\gamma)d\gamma \tag{31}$$

where A_1 and A_2 that represent the modulation parameters are given in Table 2.[2]

Substituting (24) into (31) along with the change of the order of the integrals and using the identity [28, eq. (06.27.26.0006.01)]

$$\mathrm{erfc}(\sqrt{x}) = \frac{1}{\sqrt{\pi}}G_{1,2}^{2,0}\left[x\middle|\begin{matrix}1\\0,\,0.5\end{matrix}\right] \tag{32}$$

We have (33) that is shown at the bottom of the page.

Now, one can see that the inner integral is recorded in [23, eq. (2.9)]. Subsequently, invoking the definition of the BFHF [23, eq. (2.57)], exact closed-form expression of the $\bar{P}_s^C$ can be derived as in (34) shown at the bottom of the next page.

When $\bar{\gamma} \to \infty$, the $\bar{P}_s^{C,\infty}$ can be derived via inserting (13) in (31) and utilising [28, eq. (06.27.21.0132.01)]. Thus, after

[2]For GMSK, $A_2 = B$ which is the bandwidth of the premodulation.

$$\mathcal{M}_\gamma^{(k)}(s) = \frac{\alpha\phi^\mu}{2\Gamma(\frac{\mu\varphi}{1+p})\bar{\gamma}^{\frac{\alpha\mu}{2}}}\left(\frac{p}{\eta}\right)^{\frac{\mu p}{1+p}} \times\frac{1}{(2\pi i)^2}\int_{\mathcal{T}_1}\int_{\mathcal{T}_2}\int_0^\infty \gamma^{\frac{\alpha\mu}{2}-\frac{\alpha}{2}t_1-\frac{\alpha}{2}t_2-1}e^{-s\gamma}d\gamma\frac{\Gamma(t_1)\Gamma(t_2)\Gamma\left(\frac{\mu\varphi}{1+p}-t_2\right)}{\Gamma(\mu-t_2)}\left(\frac{\phi\delta}{\bar{\gamma}^{\frac{\alpha}{2}}}\right)^{-t_1}\left(\frac{\phi\beta}{\eta\bar{\gamma}^{\frac{\alpha}{2}}}\right)^{-t_2}dt_1dt_2. \tag{28}$$

$$\bar{P}_s^C = \frac{\alpha\phi^\mu A_1}{2\sqrt{\pi}\Gamma(\frac{\mu\varphi}{1+p})\bar{\gamma}^{\frac{\alpha\mu}{2}}}\left(\frac{p}{\eta}\right)^{\frac{\mu p}{1+p}} \times\frac{1}{(2\pi i)^2}\int_{\mathcal{T}_1}\int_{\mathcal{T}_2}\int_0^\infty \gamma^{\frac{\alpha\mu}{2}-\frac{\alpha}{2}t_1-\frac{\alpha}{2}t_2-1}G_{1,2}^{2,0}\left[A_2\gamma\middle|\begin{matrix}1\\0,\,0.5\end{matrix}\right]d\gamma\frac{\Gamma(t_1)\Gamma(t_2)\Gamma\left(\frac{\mu\varphi}{1+p}-t_2\right)}{\Gamma(\mu-t_2)}\left(\frac{\phi\delta}{\bar{\gamma}^{\frac{\alpha}{2}}}\right)^{-t_1}\left(\frac{\phi\beta}{\eta\bar{\gamma}^{\frac{\alpha}{2}}}\right)^{-t_2}dt_1dt_2. \tag{33}$$

performing some mathematical simplifications, this yields

$$\bar{P}_s^{C,\infty} \simeq \frac{\phi^{\mu} A_1}{\sqrt{\pi}\Gamma(1+\mu)(A_2\bar{\gamma})^{\frac{\alpha\mu}{2}}}\left(\frac{p}{\eta}\right)^{\frac{\mu p}{1+p}}\Gamma\left(\frac{1+\alpha\mu}{2}\right). \quad (35)$$

From (35), it is clear that $\mathcal{G}_d = \alpha\mu/2$ and $\mathcal{G}_c = A_2\left[\left(\frac{\eta}{p}\right)^{p/(1+p)}\left(\frac{\sqrt{\pi}\Gamma(1+\mu)}{A_1\phi^{\mu}\Gamma((1+\alpha\mu)/2)}\right)^{\frac{1}{\mu}}\right]^{2/\alpha}$.

C. AMOUNT OF FADING AND CHANNEL QUALITY ESTIMATION INDEX

The AoF, $\mathcal{AF}$, can be computed by [26, eq. (1.27)]

$$\mathcal{AF} = \frac{\mathbb{E}[\gamma^2]}{\mathbb{E}[\gamma]^2} - 1 \quad (36)$$

where $\mathbb{E}[\gamma]$ and $\mathbb{E}[\gamma^2]$ that represent the first and second moments of γ, respectively, can be deduced from (25) via inserting $k = 2$ and $k = 1$, respectively, along with $s = 0$. Thus, after plugging (18) in (27) with $s = 0$ and performing the change of the variable $u = \gamma^{\alpha/2}$, the integral can be evaluated with the aid of [23, eq. (2.3), pp. 60]. Hence, the k-th moment of γ, $\boldsymbol{\mu}_k$, over extended $\alpha - \eta - \mu$ fading distribution is expressed as

$$\boldsymbol{\mu}_k = \mathbb{E}[\gamma^k] = \frac{\left(\frac{p}{\eta}\right)^{\frac{\mu p}{1+p}}}{\delta^{\mu}\Gamma\left(\frac{\mu\varphi}{1+p}\right)}\left(\frac{\bar{\gamma}^{\frac{\alpha}{2}}}{\phi\delta}\right)^{\frac{2k}{\alpha}} \times H_{2,2}^{1,2}\left[\frac{\beta}{\eta\delta}\middle|\begin{matrix}(1-\mu-\frac{2}{\alpha}k,\,1),\,(1-\frac{\mu\varphi}{1+p},\,1)\\(0,\,1),\,(1-\mu,\,1)\end{matrix}\right]. \quad (37)$$

Alternatively, (37) can be rewritten in terms of the hypergeometric function via recalling the identity [23, eq. (1.132)]

$$H_{2,2}^{1,2}\left[x\middle|\begin{matrix}(1-a,\,1),\,(1-b,\,1)\\(0,\,1),\,(1-c,\,1)\end{matrix}\right] = \frac{\Gamma(a)\Gamma(b)}{\Gamma(c)}{}_2F_1(a,b;c;-x). \quad (38)$$

Consequently, this yields

$$\boldsymbol{\mu}_k = \mathbb{E}[\gamma^k] = \frac{\Gamma(\mu+\frac{2}{\alpha}k)\left(\frac{p}{\eta}\right)^{\frac{\mu p}{1+p}}}{\delta^{\mu}\Gamma(\mu)}\left(\frac{\bar{\gamma}^{\frac{\alpha}{2}}}{\phi\delta}\right)^{\frac{2k}{\alpha}} \times {}_2F_1\left(\frac{\mu\varphi}{1+p},\,\mu+\frac{2}{\alpha}k;\,\mu;\,-\frac{\beta}{\eta\delta}\right). \quad (39)$$

The CQEI, $\mathcal{CQEI}$, that is defined as an effective metric that gives insights on the AoF of at a specific values of SNR, can be expressed as [29]

$$\mathcal{CQEI} = \frac{\mathcal{AF}}{\mathbb{E}[\gamma]} - 1. \quad (40)$$

D. EFFECTIVE RATE

The ER of wireless communications systems is measured under imperfect quality of service (QoS) where several restrictions such as system delay and block duration are taken into account [30].

The ER, $\mathcal{R}$ is given by [30, eq. (8)]

$$\mathcal{R} = -\frac{1}{\mathcal{A}}\log_2\left\{\int_0^{\infty}(1+\gamma)^{-\mathcal{A}}f_{\gamma}(\gamma)d\gamma\right\} \quad (41)$$

where $\mathcal{A} \triangleq \theta T\mathcal{B}/\ln(2)$ with θ represents the delay exponent whereas T and $\mathcal{B}$ indicate the time and bandwidth of the channel, respectively.

The ER over extended $\alpha - \eta - \mu$ fading model can be derived via inserting (24) in (41) and employing [22, eq. (3.194.3)] to compute the linear integral. Then, after invoking the property $B(x, y) = \Gamma(x)\Gamma(y)/\Gamma(x+y)$ [22, eq. (8.384.1)] for the beta function and using the definition of the BFHF [23, eq. (2.57)], we have (42) shown at the bottom of the page.

The asymptotic behaviour of ER at high $\bar{\gamma}$, $\mathcal{R}^{\infty}$, can be analysed by

$$\mathcal{R}^{\infty} \simeq -\frac{1}{\mathcal{A}}\log_2\left\{\frac{\alpha\phi^{\mu}}{2\Gamma(\mu)\bar{\gamma}^{\frac{\alpha\mu}{2}}}\left(\frac{p}{\eta}\right)^{\frac{\mu p}{1+p}}B\left(\frac{\alpha\mu}{2},\,\mathcal{A}-\frac{\alpha\mu}{2}\right)\right\} \quad (43)$$

where (43) arises after substituting (13) into (41) and making use of [22, eq. (3.194.3)].

E. AVERAGE CHANNEL CAPACITY UNDER DIFFERENT ADAPTIVE TRANSMISSION PROTOCOLS

1) OPTIMUM RATE ADAPTATION WITH CONSTANT TRANSMIT POWER

The normalized ACC under ORA strategy, $\bar{C}_{ORA}$, can be determined by [31, eq. (20)]

$$\bar{C}_{ORA} = \frac{1}{\ln(2)}\int_0^{\infty}\ln(1+\gamma)f_{\gamma}(\gamma)d\gamma. \quad (44)$$

Substituting (20) into (44) and changing the order of the integrals to evaluate the linear integral with the help of [22, eq.(4.293.3)]. Furthermore, recalling the identity $\Gamma(1-z)\Gamma(z) = \pi/\sin(\pi z)$ [22, eq. (8.334.3)] and using [23, eq.

$$\bar{P}_s^{C} = \frac{\alpha\phi^{\mu}A_1}{2\sqrt{\pi}\Gamma(\frac{\mu\varphi}{1+p})(A_2\bar{\gamma})^{\frac{\alpha\mu}{2}}}\left(\frac{p}{\eta}\right)^{\frac{\mu p}{1+p}}H_{2,1:0,1;1,1;1,2}^{0,2:1,0;1,1}\left[\frac{\phi\delta}{(A_2\bar{\gamma})^{\frac{\alpha}{2}}},\frac{\phi\beta}{\eta(A_2\bar{\gamma})^{\frac{\alpha}{2}}}\middle|\begin{matrix}(\frac{1}{2}-\frac{\alpha\mu}{2};\frac{\alpha}{2},\frac{\alpha}{2}),(1-\frac{\alpha\mu}{2};\frac{\alpha}{2},\frac{\alpha}{2}):-;(1-\frac{\mu\varphi}{1+p},1)\\(-\frac{\alpha\mu}{2};\frac{\alpha}{2},\frac{\alpha}{2}):(0,1);(0,1),(1-\mu,1)\end{matrix}\right]. \quad (34)$$

$$\mathcal{R} = -\frac{1}{\mathcal{A}}\log_2\left\{\frac{\alpha\phi^{\mu}}{2\Gamma(\mathcal{A})\Gamma(\frac{\mu\varphi}{1+p})\bar{\gamma}^{\frac{\alpha\mu}{2}}}\left(\frac{p}{\eta}\right)^{\frac{\mu p}{1+p}}H_{1,1:0,1;1,2}^{1,1:1,0;1,1}\left[\frac{\phi\delta}{\bar{\gamma}^{\frac{\alpha}{2}}},\frac{\phi\beta}{\eta\bar{\gamma}^{\frac{\alpha}{2}}}\middle|\begin{matrix}(1-\frac{\alpha\mu}{2};\frac{\alpha}{2},\frac{\alpha}{2}):-;(1-\frac{\mu\varphi}{1+p},1)\\(\mathcal{A}-\frac{\alpha\mu}{2};\frac{\alpha}{2},\frac{\alpha}{2}):(0,1);(0,1),(1-\mu,1)\end{matrix}\right]\right\}. \quad (42)$$

(2.57)] to write $\bar{C}_{ORA}$ in exact closed-form expression as in (45) shown at the bottom of the page.

2) CHANNEL INVERSION AND FIXED RATE

The normalized ACC with CIFR, $\bar{C}_{CIFR}$, can be computed by [31, eq. (73)]

$$\bar{C}_{CIFR} = \log_2\left\{1 + \left(\int_0^\infty \gamma^{-1} f_\gamma(\gamma) d\gamma\right)^{-1}\right\}. \quad (46)$$

The integral of (46) can be obtained from (37) or (39) via setting $k = -1$.

3) TRUNCATED INVERSION AND FIXED RATE

The normalized ACC with TIFR, $\bar{C}_{TIFR}$, can be calculated by [31, eq. (85)]

$$\bar{C}_{TIFR} = \log_2\left\{1 + \left(\int_{\gamma_0}^\infty \gamma^{-1} f_\gamma(\gamma) d\gamma\right)^{-1}\right\}(1 - F_\gamma(\gamma_0)) \quad (47)$$

where γ_0 is a certain threshold value that is selected to achieve maximum $\bar{C}_{TIFR}$.

The integral of (47) can be rewritten as

$$\int_{\gamma_0}^\infty \gamma^{-1} f_\gamma(\gamma) d\gamma = I_1 - I_2 \quad (48)$$

where

$$I_1 = \int_0^\infty \gamma^{-1} f_\gamma(\gamma) d\gamma$$

and

$$I_2 = \int_0^{\gamma_0} \gamma^{-1} f_\gamma(\gamma) d\gamma.$$

It can be observed that I_1 can be deduced from (37) or (39) with $k = -1$. In addition, I_2 can be derived via following the same procedure of the CDF in Theorem 2 to yield (49) given at the bottom of the page.

V. NUMERICAL AND SIMULATION RESULTS

In this section, the numerical results for different scenarios are presented to understand the impact of the fading parameters α and p of the extended α-η-μ fading distribution on the performance metrics of the wireless communications systems. In addition, to verify the validation of the derived expressions, the analytical results are compared with the Monte Carlo simulations that are generated via using 10^7 realizations. To achieve further validations for our

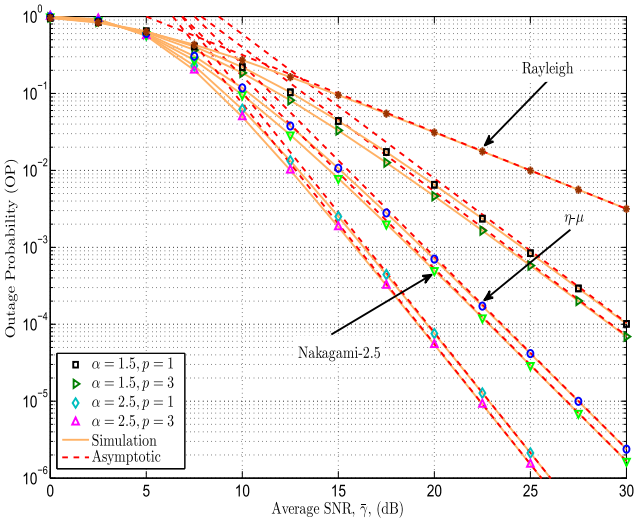

FIGURE 3. Exact and asymptotic OP versus $\bar{\gamma}$ over extended $\alpha - \eta - \mu$ fading for $\psi = 5$ dB, $\eta = 3$, $\mu = 2.5$, and arbitrary values of α and p.

derived expressions, several comparisons with some special cases of extended α-η-μ fading, such as, η-μ and Nakagami-2.5, that were investigated in the previous works, have been carried out.[3] In all figures, the markers stand for the numerical results, whereas the solid and dashed lines denote their simulation and asymptotic counterparts, respectively. Moreover, in this work, the parameters η and μ are assumed to be constant where $\eta = 3$ and $\mu = 2.5$. This is because the influence of these parameters has been widely studied in the literature (please refer to [1], [3], [6], [8], [11], and [17]).

Figs. 3 and 4 demonstrate the OP with $\psi = 5$ dB and ASEP for DBPSK modulation, respectively, versus average SNR, $\bar{\gamma}$, over extended $\alpha - \eta - \mu$ fading model for arbitrary values of α and p. As expected, both figures explain that the OP and ASEP diminish when α or/and p increase. This is because the increasing in α leads to high power exponent of the sum of multipath components. On the other side, the increasing in p means the number of the multipath clusters of the in-phase components is higher than that of the quadrature components of the same signal. For instance, in Figs. 3 and 4, when α changes from 1.5 to 2.5 at $p = 1$ (fixed) and $\bar{\gamma} = 15$ dB (fixed), the OP is reduced by approximately 94% and

[3]The MATLAB codes for the special cases of the extended α-η-μ fading, such as η-μ and α-μ models are implemented in [32] whereas for extended α-η-μ fading, we have developed the MATLAB code that is available at: https://github.com/hugerles/extended.git.

$$\bar{C}_{ORA} = \frac{\alpha\phi^\mu}{2\ln(2)\Gamma(\frac{\mu\varphi}{1+p})\bar{\gamma}^{\frac{\alpha\mu}{2}}}\left(\frac{p}{\eta}\right)^{\frac{\mu p}{1+p}} H^{1,2:1,0;1,1}_{2,2:0,1;1,2}\left[\frac{\phi\delta}{\bar{\gamma}^{\frac{\alpha}{2}}}, \frac{\phi\beta}{\eta\bar{\gamma}^{\frac{\alpha}{2}}}\middle| \begin{matrix}(1-\frac{\alpha\mu}{2};\frac{\alpha}{2},\frac{\alpha}{2}),(1-\frac{\alpha\mu}{2};\frac{\alpha}{2},\frac{\alpha}{2}):-;(1-\frac{\mu\varphi}{1+p},1)\\ (1-\frac{\alpha\mu}{2};\frac{\alpha}{2},\frac{\alpha}{2}),(-\frac{\alpha\mu}{2};\frac{\alpha}{2},\frac{\alpha}{2}):(0,1);(0,1),(1-\mu,1)\end{matrix}\right]. \quad (45)$$

$$I_2 = \frac{\alpha\phi^\mu}{2\Gamma(\frac{\mu\varphi}{1+p})}\left(\frac{p}{\eta}\right)^{\frac{\mu p}{1+p}} \frac{\gamma_0^{\frac{\alpha\mu}{2}-1}}{\bar{\gamma}^{\frac{\alpha\mu}{2}}} H^{0,1:1,0;1,1}_{1,1:0,1;1,2}\left[\frac{\phi\delta}{\bar{\gamma}^{\frac{\alpha}{2}}}\gamma_0^{\frac{\alpha}{2}}, \frac{\phi\beta}{\eta\bar{\gamma}^{\frac{\alpha}{2}}}\gamma_0^{\frac{\alpha}{2}}\middle| \begin{matrix}(2-\frac{\alpha\mu}{2};\frac{\alpha}{2},\frac{\alpha}{2}):-;(1-\frac{\mu\varphi}{1+p},1)\\ (1-\frac{\alpha\mu}{2};\frac{\alpha}{2},\frac{\alpha}{2}):(0,1);(0,1),(1-\mu,1)\end{matrix}\right]. \quad (49)$$

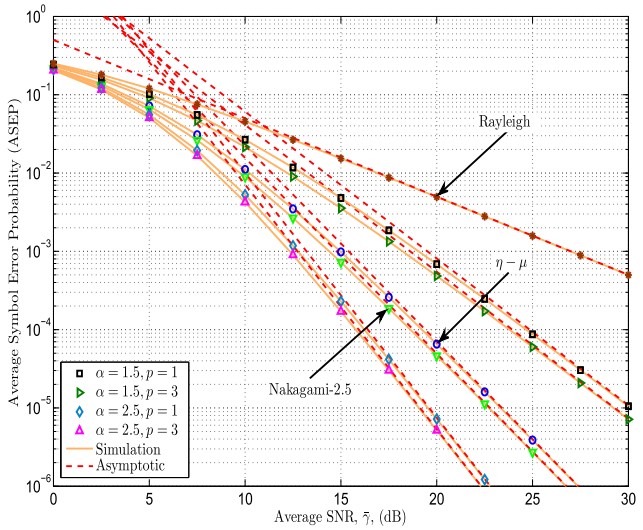

FIGURE 4. Exact and asymptotic ASEP of DBPSK versus $\bar{\gamma}$ over extended $\alpha-\eta-\mu$ fading for $\eta=3$, $\mu=2.5$, and arbitrary values of α and p.

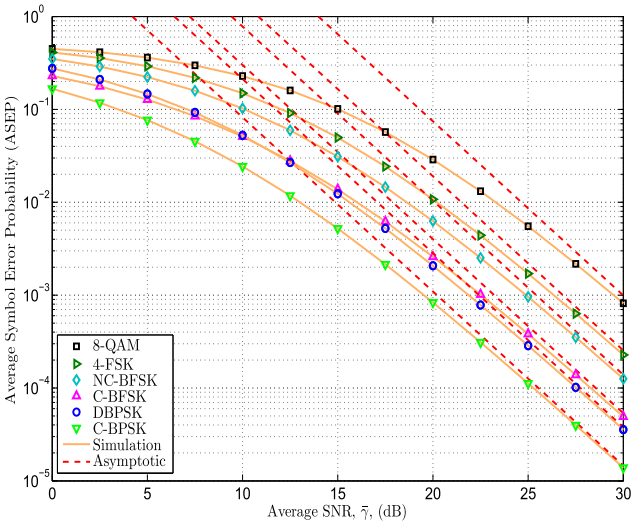

FIGURE 5. Exact and asymptotic ASEP of various schemes versus $\bar{\gamma}$ over extended $\alpha-\eta-\mu$ fading for $\alpha=1.5$, $\eta=3$, $\mu=2.5$, and $p=0.3$.

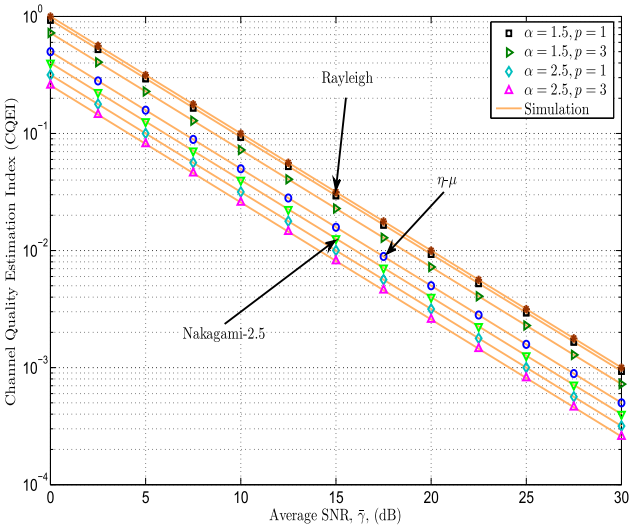

FIGURE 6. CQEI versus $\bar{\gamma}$ over extended $\alpha-\eta-\mu$ fading for $\alpha=1.5$, $\eta=3$, $\mu=2.5$, and $p=0.3$.

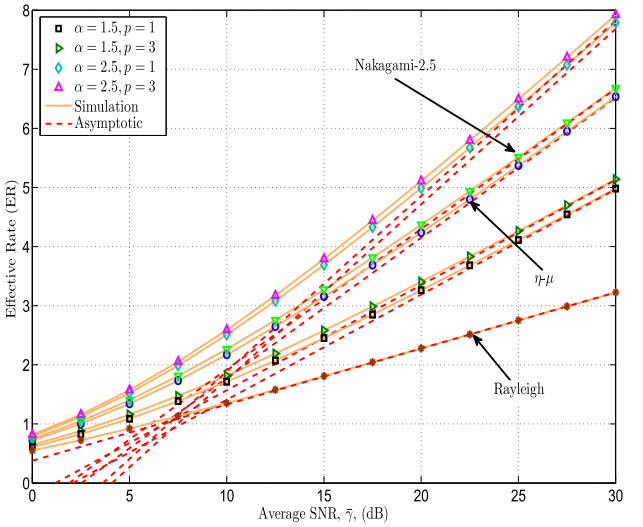

FIGURE 7. Exact and asymptotic ER versus $\bar{\gamma}$ over extended $\alpha-\eta-\mu$ fading for $\eta=3$, $\mu=2.5$, $\mathcal{A}=3.5$ and arbitrary values of α and p.

the ASEP is decreased by nearly 95%. In the same context, at constant $\bar{\gamma}=15$ dB and $\alpha=2.5$, the OP and ASEP for $p=3$ are roughly 27% and 30%, respectively, less than that of $p=1$. However, the effect of α on the performance measures is more pronounced of that of p. This confirms the correctness of our derived expressions of the diversity gain for both the OP and ASEP that is proportional to α and μ, namely, $\mathcal{G}_d=\alpha\mu/2$. Hence, the overall system performance greatly degrades with the dropping in the value of α and vice versa.

Fig. 5 depicts the exact and asymptotic results of the ASEP for various modulation schemes versus average SNR, $\bar{\gamma}$, for $\alpha=1.5$ and $p=0.3$. As anticipated and widely presented in the technical literature, the C-BPSK scheme outperforms the other formats. On the contrary, the 8-QAM technique has higher ASEP than that of 4-FSK, NC-BFSK, C-BFSK, and DBPSK schemes.

Fig. 6 plots the CQEI versus average SNR, $\bar{\gamma}$, over extended $\alpha-\eta-\mu$ fading for different values of α and p. As it can noted, in this figure, that the CQEI drops when α or/and p increase. This is because the AoF diminishes as α or/and p become high.

Fig. 7 shows the exact and asymptotic results of the ER versus average SNR, $\bar{\gamma}$, over extended $\alpha-\eta-\mu$ fading for $\mathcal{A}=3.5$ and arbitrary numbers of α and p. Similar to Figs. 3 and 4 as well as for the same reasons, the ER improves when α or/and p become large. For example, at $p=1$ (fixed) and $\bar{\gamma}=15$ dB (fixed), the ER for $\alpha=2.5$ is roughly increased by 50% when compared to $\alpha=1.5$. In the same

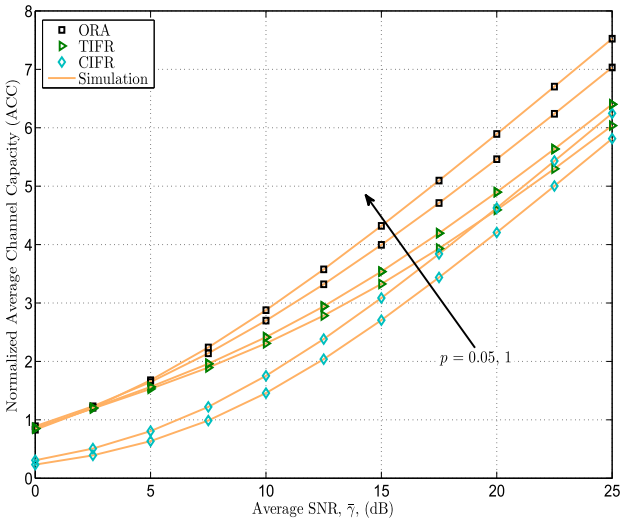

FIGURE 8. ACC for different transmission policies versus $\bar{\gamma}$ over extended $\alpha - \eta - \mu$ fading with $\eta = 3$, $\mu = 2.5$, $\alpha = 1.5$ and arbitrary values of p.

context, the ER for $p = 3$ is nearly improved by 2.8% when compared to $p = 1$ at constant $\alpha = 2.5$.

It is worth mentioning that the influence of p on the ACC with different transmission strategies has not been studied in [17] and [21]. Hence, Fig. 8 illustrates the normalized ACC with ORA, TIFR, and CIFR transmission techniques over extended $\alpha - \eta - \mu$ fading model for $\alpha = 1.5$, $p = 0.05$, and $p = 1$. From this figure, it is clear that as p increases, the ACC becomes high and for the same reason that has been shown for the results of Figs. 3 and 4. Furthermore, the ORA has the superiority on the TIFR which is better than CIFR. These observations are consistent with the results of [3] and [12] which prove the correctness of the provided expressions in this work.

For further insights about the proposed fading model, Figs. 3, 4, 6, and 7 also include the results for η-μ, Nakagami-2.5, and Rayleigh fading channels that are special cases of the extended $\alpha - \eta - \mu$ fading model as previously explained in Table 1. From these figures, it can be noted that the metrics over the extended $\alpha - \eta - \mu$ fading condition with $\alpha = 2.5$ have better performance than the Nakagami-2.5 fading channel. This refers to the low value of α of the Nakagami-2.5 fading condition ($\alpha = 2$). This provides another confirmation about the influence of the non-linearity of the propagation media on the system behaviour. Besides, one can see that the system has worse performance over Rayleigh fading channel. This is because the number of the multipath clusters of the Rayleigh fading channel that arrives at the receiver is 1 ($\mu = 1$) whereas $\mu = 2.5$ for the extended $\alpha - \eta - \mu$ fading model and Nakagami-2.5. Therefore, the performance metrics over Rayleigh fading channel have lower diversity gain in comparison with the other scenarios. Also, it is obvious, in all figures, that the numerical results are in excellent matching with the asymptotic behaviour at high average SNR, $\bar{\gamma}$, as well as the Monte Carlo simulations.

VI. CONCLUSION

This paper was devoted to analyse the impact of the non-linearity propagation environment on the extended η-μ fading distribution. Accordingly, the extended α-η-μ fading was proposed as a new fading model via deriving the exact and asymptotic expressions of the PDF, CDF, and G-MGF of both the signal envelope and instantaneous SNR. Based on these statistics, exact closed-form mathematically tractable expressions of the OP, ASEP for different modulation formats, AoF, CQEI, and ER were provided. Moreover, the asymptotic expressions at high average SNR of the OP, ASEP, and ER were also given. Additionally, the analysis of the ACC with ORA, CIFR, and TIFR transmission protocols was presented. From the presented results, a degradation in the performance metrics can be noticed when α or/and p reduce. However, the parameter α has higher impact than p and this has been proved by the diversity gain which is proportional to α. A comparison between the numerical results and Monte Carlo simulation was performed to verify the validation of the derived expressions. The derived expressions of this work can be applied for number of fading channels that are special cases of the extended α-η-μ fading model. For instance, the performance analysis of the wireless communications systems over Nakagami-m fading channel with better fitting to the practical data than the classical model can be obtained by using the extended α-η-μ fading condition with the fading parameters of Table 1. In addition, the ACC with different adaptive power transmission policies over extended η-μ fading that has not been yet analysed in the literature, can be studied by utilising the expressions of Section IV.E after inserting $\alpha = 2$.

REFERENCES

[1] M. D. Yacoub, "The κ-μ distribution and the η-μ distribution," *IEEE Antennas Propag. Mag.*, vol. 49, no. 1, pp. 68–81, Feb. 2007.
[2] M. D. Yacoub, "The α-μ distribution: A physical fading model for the Stacy distribution," *IEEE Trans. Veh. Technol.*, vol. 56, no. 1, pp. 27–34, Jan. 2007.
[3] J. Zhang et al., "Performance analysis of digital communication systems over composite η-μ/gamma fading channels," *IEEE Trans. Veh. Technol.*, vol. 61, no. 7, pp. 3114–3124, Sep. 2012.
[4] G. Fraidenraich and M. D. Yacoub, "The α-η-μ and α-κ-μ fading distributions," in *Proc. IEEE Int. Symp. Spread Spectr. Techn. Appl. (ISSSTA)*, Manaus, Brazil, Oct. 2006, pp. 16–20.
[5] E. Salahat and A. Hakam, "Performance analysis of α-η-μ and α-κ-μ generalized mobile fading channels," in *Proc. Eur. Wireless, 20th Eur. Wireless Conf.*, May 2014, pp. 1–6.
[6] O. S. Badarneh and M. S. Aloqlah, "Performance analysis of digital communication systems over α-η-μ fading channels," *IEEE Trans. Veh. Technol.*, vol. 65, no. 10, pp. 7972–7981, Oct. 2016.
[7] M. Bhatt and S. K. Soni, "Energy detection over unified α-η-μ and α-κ-μ fading channels," in *Proc. Int. Conf. Inventive Commun. Comput. Technol. (ICICCT)*, Apr. 2018, pp. 1269–1272.
[8] V. K. Upadhaya, P. S. Chauhan, and S. K. Soni, "Effective capacity analysis over generalized α-η-μ fading channel," in *Proc. Int. Conf. Electr., Electron. Comput. Eng. (UPCON)*, 2019, pp. 1–3.
[9] J. M. Moualeu, D. B. D. Costa, W. Hamouda, U. S. Dias, and R. A. A. D. Souza, "Physical layer security over α-η-μ and α-κ-μ fading channels," *IEEE Trans. Veh. Technol.*, vol. 68, no. 1, pp. 1025–1029, Jan. 2019.
[10] V. A. Aalo, P. S. Bithas, and G. P. Efthymoglou, "Ergodic capacity of generalized fading channels with mobility," *IEEE Open J. Veh. Technol.*, vol. 3, pp. 15–25, 2022.

[11] H. Al-Hmood and H. S. Al-Raweshidy, "Unified approaches based effective capacity analysis over composite /gamma fading channels," *Electron. Lett.*, vol. 54, no. 13, pp. 852–853, Jun. 2018.

[12] H. Al-Hmood and H. S. Al-Raweshidy, "Unified analysis of channel capacity under different adaptive transmission policies," *Electron. Lett.*, vol. 56, no. 2, pp. 87–89, Jan. 2020.

[13] M. D. Yacoub, "The α-η-κ-μ fading model," *IEEE Trans. Antennas Propag.*, vol. 64, no. 8, pp. 3597–3610, Aug. 2016.

[14] A. A. Dos Anjos, "Higher order statistics in a mmWave propagation environment," *IEEE Access*, vol. 7, pp. 103876–103892, 2019.

[15] H. Al-Hmood and H. S. Al-Raweshidy, "On the effective rate and energy detection based spectrum sensing over α-η-κ-μ fading channels," *IEEE Trans. Veh. Technol.*, vol. 69, no. 8, pp. 9112–9116, Aug. 2020.

[16] Y. Ai, A. Mathur, L. Kong, and M. Cheffena, "Effective throughput analysis of α-η-κ-μ fading channels," *IEEE Access*, vol. 8, pp. 57363–57371, 2020.

[17] G. R. D. L. Tejerina, C. R. N. D. Silva, and M. D. Yacoub, "Extended η-μ fading models," *IEEE Trans. Wireless Commun.*, vol. 19, no. 12, pp. 8153–8164, Dec. 2020.

[18] O. S. Badarneh and F. S. Almehmadi, "On the sum of extended η-μ variates with MRC applications," *IEEE Commun. Lett.*, vol. 25, no. 11, pp. 3518–3522, Nov. 2021.

[19] O. S. Badarneh, M. K. Alshawaqfeh, F. S. Almehmadi, and H. S. Silva, "Selection combining over the extended η-μ fading channels," *IEEE Wireless Commun. Lett.*, vol. 11, no. 4, pp. 722–726, Apr. 2022.

[20] Z. Hussain, H. Mehdi, and S. M. A. Saleem, "Relay-assisted D2D communication over extended η-μ fading channels," *Mobile Inf. Syst.*, vol. 2022, pp. 1–14, Mar. 2022.

[21] H. Silva, O. Badarneh, and W. J. L. Queiroz, "The extended η-$\mathcal{F}$ composite fading distribution," *IEEE Trans. Veh. Technol.*, vol. 71, no. 9, pp. 10104–10109, May 2022.

[22] I. S. Gradshteyn and I. M. Ryzhik, *Table of Integrals, Series and Products*, 7th ed. New York, NY, USA: Academic, 2007.

[23] A. M. Mathai, R. K. Saxena, and H. J. Haubold, *The H-Function: Theory and Applications*, 1st ed. New York, NY, USA: Springer, 2009.

[24] K. P. Peppas, "A new formula for the average bit error probability of dual-hop amplify-and-forward relaying systems over generalized shadowed fading channels," *IEEE Wireless Commun. Lett.*, vol. 1, no. 2, pp. 85–88, Apr. 2012.

[25] J. P. Peña-Martín, J. M. Romero-Jerez, and F. J. Lopez-Martinez, "Generalized MGF of Beckmann fading with applications to wireless communications performance analysis," *IEEE Trans. Commun.*, vol. 65, no. 9, pp. 3933–3943, Sep. 2017.

[26] M. K. Simon and M.-S. Alouini, *Digital Communications Over Fading Channels*. New York, NY, USA: Wiley, 2005.

[27] N. C. Sagias, D. A. Zogas, and G. K. Karagiannidis, "Selection diversity receivers over nonidentical Weibull fading channels," *IEEE Trans. Veh. Technol.*, vol. 54, no. 6, pp. 2146–2151, Nov. 2005.

[28] *Wolfram Research*. Accessed: Jun. 2021. [Online]. Available: https://content.wolfram.com/uploads/sites/39/2015/02/MathematicalNotation-SW.pdf

[29] A. S. Lioumpas, G. K. Karagiannidis, and A. C. Iossifides, "Channel quality estimation index (CQEI): A long-term performance metric for fading channels and an application in EGC receivers," *IEEE Trans. Wireless Commun.*, vol. 6, no. 9, pp. 3315–3323, Sep. 2007.

[30] S. K. Yoo, S. L. Cotton, P. C. Sofotasios, S. Muhaidat, and G. K. Karagiannidis, "Effective capacity analysis over generalized composite fading channels," *IEEE Access*, vol. 8, pp. 123756–123764, 2020.

[31] S. K. Yoo et al., "A comprehensive analysis of the achievable channel capacity in $\mathcal{F}$ composite fading channels," *IEEE Access*, vol. 7, pp. 34078–34094, 2019.

[32] B. Kumbhani and R. S. Kshetrimayum, *MIMO Wireless Communications Over Generalized Fading Channels*, 1st ed. FL, USA: Taylor & Francis Group, 2017.

HUSSIEN AL-HMOOD (Member, IEEE) received the B.S. and M.Sc. degrees in electrical and electronic engineering from the University of Baghdad, Baghdad, Iraq, in 2005 and 2007, respectively, and the Ph.D. degree from Brunel University London, London, U.K., in 2015. From November 2016 till October 2018, he was the Head of the Electrical and Electronic Engineering (EEE). He is currently an Assistant Professor at the EEE Department, University of Thi-Qar, Thi-Qar, Iraq. He has participated in many international conferences and published number of articles in high quality journals such as IEEE and IET. His current research interests include estimation and detection techniques such as energy detection, cognitive radio and cooperative communications networks, diversity combining and MIMO systems, statistical characterizations of generalized composite fading channels, security of physical layer, coexistence techniques between Wi-Fi and LAA, and channel model of mmWave for 5G. In 2017, he was awarded the Fulbright USA Scholar Grant to Visit the University of Delaware, Delaware, USA. He has served as a Reviewer for many high quality journals such as IEEE TRANSACTIONS ON VEHICULAR TECHNOLOGY, IEEE WIRELESS COMMUNICATIONS LETTERS, *Electronics Letters*, IEEE COMMUNICATIONS LETTERS, IEEE ACCESS, and IEEE TRANSACTIONS ON COMMUNICATIONS.

RAFED SABBAR ABBAS received the M.Sc. and Ph.D. degrees from South Bank University and Brunel University London, London, U.K., respectively. He is currently an Associate Professor at the Electrical Engineering (EE) Department, Faculty of Engineering, University of Kufa, Iraq. He has published several articles in high quality journals such as IEEE and IET. His research interests include optical fiber, multicasting approaches, statistical characterizations of fading channels, and mmWave for 5G.

HAMED AL-RAWESHIDY (Senior Member, IEEE) received the Ph.D. degree from the University of Strathclyde, Glasgow, U.K., in 1991. He was with the Space and Astronomy Research Centre, Iraq; PerkinElmer, USA; Carl Zeiss, Germany; British Telecom, U.K.; Oxford University; Manchester Metropolitan University; and Kent University. He is currently the Director of the Wireless Networks and Communications Centre (WNCC) and the Director of PG studies at the Department of Electronic and Electrical Engineering, Brunel University London. WNCC is the largest centre at Brunel University London and one of the largest Communication Research Centre in U.K. He acts as a Consultant and involved in projects with several companies and operators such as Vodafone, U.K.; Ericsson, Sweden; Andrew, USA; NEC, Japan; Nokia, Finland; Siemens, Germany; Franc Telecom, France; Thales, U.K., and France; and Tekmar, Italy. He is a Principal Investigator for several EPSRC projects and European project such as MAGNET EU project (IP) (2004–2008). He has published over 450 papers in international journals and refereed conferences. His current research interests include 5G and beyond such as C-RAN, SDN, the IoT, M2M, and radio over fiber. He is an Editor of the first book in radio over fiber technologies for mobile communications networks.